TURBULENT HEAT TRANSFER AT THE FORWARD FACE SURFACE OF A VORTEX CHAMBER

É. P. Volchkov, S. V. Semenov, and V. I. Terekhov

UDC 532.59.001.572

We present the results from a theoretical and experimental investigation into the turbulent transfer that takes place in the face boundary layer of a vortex chamber. It is demonstrated that the intensity of heat transfer at the faces of the chamber, in view of the three-dimensional nature of the flow, is significantly greater than in the case of a standard boundary layer at a plate.

We are familiar with the fact that face boundary layers may exert significant influence on the aerodynamics of vortex chambers. The experimental and theoretical studies [1-5] are devoted to a solution of this problem. Until recently, no investigations were conducted into the transfer of heat in such boundary layers; an existing paper [6] is devoted to the study of heat and mass transfer in a laminar face layer.

The boundary layers formed at the face surfaces of vortex chambers are three-dimensional in nature. The pressure gradient along the radius of the chamber, caused by the rotation of the flow, leads to a secondary radial flow in the vicinity of the wall, and this flow is directed toward the axis of the chamber. Boundary layers in curvilinear channels exhibit a similar structure, as do those on airplane wings, the leading interblade surfaces of gas turbines, and increasing attention has recently been devoted to the study of these boundary layers [7]. Therefore, the results obtained in this paper are also of interest in studying the heat and mass transfer in three-dimensional boundary layers with twisted streamlines and, in particular, for the interaction of vortex flows and surfaces.

1. Formulation of the Problem. Integral Relationships between Energy and the Law of Heat Transfer in the Case of a Face Boundary Layer. Let us examine the boundary layer that is formed on a plane face surface of a vortex chamber (Fig. 1). As demonstrated by aerodynamic studies [4, 5, 8], in a face layer the velocity profile V in the circular direction represents a typical layer with a shear thickness δ. The velocity profile U of the secondary radial flow is similar to the distribution of velocity in the heated stream near the wall with a general thickness δ and a dimension δ_m for the portion at the wall. Consequently, the total velocity V_Σ and its direction $\varphi = \arctan U/V$ change through the height of the layer.

Let us write the equation for the transfer of heat in the boundary layer for the case of steady axisymmetric streamlining by a rotating incompressible flow with constant physical properties about an impermeable surface under conditions that are close to the isothermal $\psi = T_w/T_0 \to 1$:

$$U\frac{\partial T}{\partial r} + W\frac{\partial T}{\partial z} = \frac{\partial q}{\partial z}. \tag{1}$$

In writing (1) we assume that the transfer of heat in the longitudinal (radial) direction was considerably smaller than in the lateral (axial) direction: $\partial q/\partial r \ll \partial q/\partial z$. In the assumption that the thermal boundary layer is equal to the thickness of the hydrodynamics boundary layer, i.e., $\delta_t = \delta$, let us integrate expression (1) with consideration of the continuity equation for the following boundary conditions:

$$z = 0: U = W = V = 0;\quad T = T_w;\quad q = q_w;\quad z = \delta_t = \delta: U = U_0 \approx 0;$$
$$W = 0;\quad V = V_0;\quad T = T_0;\quad q = 0.$$

After transformation, we obtain the integral relationship for energy in the form

Thermophysics Institute, Siberian Branch, Academy of Sciences of the USSR, Novosibirsk.
Translated from Inzhenerno-Fizicheskii Zhurnal, Vol. 56, No. 2, pp. 181-188, February, 1989. Original article submitted September 28, 1987.

0022-0841/89/5602-0109$12.50

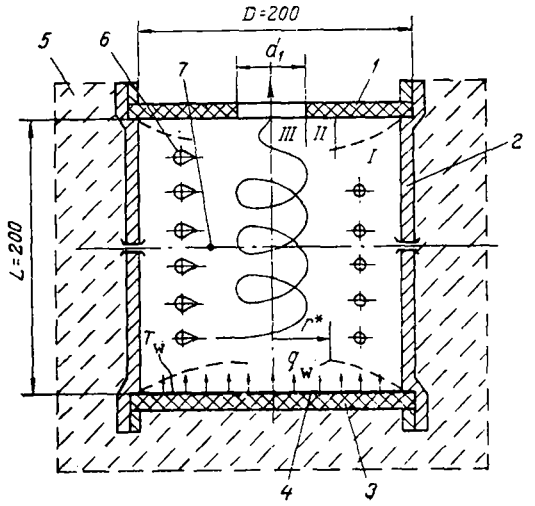

Fig. 1. Flow diagram in vortex chamber: 1) outlet face; 2) side cylinder wall; 3) heated face; 4) current-conducting layer; 5) thermal insulation; 6) orifice for entry of gas into chamber; 7) thermocouples to measure temperature fields within the chamber; I) flowthrough zones; II) non-flowthrough zone; III) outlet orifice region.

$$\frac{1}{\bar{r}\Delta T_0}\frac{d(\mathrm{Re}_t^{**}\Delta T_0\bar{r})}{d\bar{r}} = -\mathrm{St}\frac{U_m R}{\nu}. \qquad (2)$$

For the solution of Eq. (2) we must know the change along the chamber radius of the maximum value of the radial velocity U_m and we have to determine the heat-exchange law which links the Stanton number to the integral characteristics of the boundary layer. Articles [1-5, 8] examine the quantitative relationships governing the development of a face layer and its influence on the flow in the main volume of the chamber. It has been established that in the region outside of the boundary layers the entire flow can be divided into three zones along the radius of the chamber (Fig. 1). In zone I, referred to as the flowthrough zone ($\bar{r}^* < \bar{r} < 1$), the radial velocity in the core of the flow is different from zero $U_0 \neq 0$, while $\bar{r}^*$ is the boundary radius where the entire stream of gas flows into the face boundary layers and U_0 becomes equal to zero. The non-flowthrough zone II lies in the interval $\bar{r}_1 < \bar{r} < \bar{r}^*$, in which there is no radial gas flow in the region outside of the boundary layers. The third zone, i.e., $0 < \bar{r} < \bar{r}_1$, is bounded by the radius of the outlet orifice $\bar{r}_1$ through which the gas is ejected from the chamber.

Formulas have been derived in [5, 8] for the distribution, in the flowthrough zone, of the maximum radial velocity U_m in proportion to the development of the face layer along the chamber radius:

$$m \neq 0: \quad U_m/V_c = \sqrt{0.4(\bar{r}^{-2m}-1)/m}, \quad m = 0: \quad U_m/V_c = \sqrt{0{,}8\ln(1/\bar{r})}. \qquad (3)$$

We should stress that formulas (3) for the conditions of these experiments yield good agreement with the experiment conducted for the non-flowthrough zone. These expressions were therefore used subsequently for a calculation analysis and for the generalization of the experimental data relating to the transfer of heat throughout the entire chamber, excluding only the region of the outlet orifice ($\bar{r} < \bar{r}_1$).

The quantity m in formula (3) characterizes the change in the circular velocity along the radius in the core of the flow:

$$V_0 = V_c\bar{r}^{-m}. \qquad (4)$$

With m = 1, 0, and −1, respectively, we obtain rotation with constant circulation $\Gamma_0 = V_c R = Vr = \text{const}$, circular velocity $V_0 = V_c = \text{const}$, and angular velocity $\omega = V/r = V_c/R = \text{const}$.

The law governing exchange of heat in the face boundary layer will be determined from an analogy of the transfer processes for energy and angular momentum. We will assume that

the temperature and circular-velocity profiles are similar to each other, i.e., $V/V_0 = \Theta$, which is confirmed by experimental data for rotating disks [9].

In conclusion we have the following expression for the heat-transfer coefficient [8]:

$$St = \frac{q_w}{\rho C_p U_m \Delta T_0} = St\Psi_\varphi = \frac{B}{2} Re_t^{**-m_1} Pr^{m_1-1} \Psi_\varphi. \quad (5)$$

For developed turbulent flow B = 0.0256; m_1 = 0.25. In formula (5) $\Psi\varphi = [(1 + \tan^2\varphi_w)/\tan^2\varphi_w]^{3/8}$ is the heat-transfer function which describes the effect of the three-dimensional flow on intensification of heat exchange. It can easily be demonstrated that near the wall ($0 < z < \delta_m$) the magnitude of the twisting angle through the thickness of the boundary layer is constant and equal to the value at the wall, i.e., φ_w. According to the data of [5, 8], the distribution of the twisting angle at the wall along the radius of the face surface is described by the following:

$$m \neq 0: \operatorname{tg}\varphi_w = 0.83\bar{r}^m[(\bar{r}^{-2m} - 1)/m]^{1/2}, \quad m = 0: \operatorname{tg}\varphi_w = 1.17[\ln(1/\bar{r})]^{1/2}. \quad (6)$$

With relationship (6) we can calculate the change in the heat-exchange function Ψ_φ along the radius of the face surface. The range of variations in the function Ψ_φ is substantial: its magnitude depends both on the radius and on the distribution of the circular velocity outside of the boundary layer. Calculations have shown that the extensiveness of the flow exerts the greatest influence on the heat and mass transfer in the case of the potential (m = 1) law governing gas rotation above the boundary layer. The heat-exchange function Ψ_φ increases in the direction of the periphery of the chamber, where the radial velocity component is not great, $\tan\varphi_w = U_m/V_m \to 0$, and the circular velocity component predominates.

With a constant heat flux q_w = const at the wall under the condition $Re_t^{**} = 0$ when $\bar{r} = 1$, after integration of relationship (2) we have

$$Re_t^{**} = -\frac{1}{\Delta T_0 \bar{r}_1} \int_1^{\bar{r}} \frac{R}{\rho C_p \nu} q_w \bar{r}\, d\bar{r} = \Psi_\varphi St_0 \frac{1-\bar{r}^2}{2\bar{r}} Re_c \frac{U_m}{\bar{V}_c}. \quad (7)$$

Using expressions (3), (5)-(7), we obtain the calculation relationships for the Stanton number

$$St = 0.0431 \frac{[m + 0.69(1-\bar{r})^{2m}]^{0.3}(1-\bar{r}^2)^{-0.2}}{(1-\bar{r}^{2m})^{0.4}\bar{r}^{-0.2(m+1)}m^{-0.1}} Pr^{-0.6} Re_c^{-0.2} \quad (8)$$

and the heat-transfer coefficient

$$\alpha = 0.027 \frac{[m + 0.69(1-\bar{r}^{2m})]^{0.3}(1-\bar{r}^{2m})^{0.1}}{(1-\bar{r}^2)^{0.2}\bar{r}^{0.2(4m-1)}m^{0.4}} \rho C_p V_c Re_c^{-0.2} Pr^{-0.6}. \quad (9)$$

Accordingly, the Reynolds number constructed through the energy-loss thickness is determined by

$$Re_t^{**} = 0.0136 \frac{[m + 0.69(1-\bar{r}^{2m})]^{0.3}(1-r^2)^{0.8}}{\bar{r}^{0.8(m+1)}m^{0.4}(1-\bar{r}^{2m})^{-0.1}} Re_c^{0.8} Pr^{-0.6}. \quad (10)$$

Thus, Eqs. (8)-(10) allow us to calculate the transfer of heat in the turbulent face layer for any distribution of the circular velocity along the radius of the vortex chamber. In analogous fashion we can also solve the problem for the boundary condition T_w = const; the calculated relationships for this case are presented in [8].

2. Experimental Investigation of Heat Transfer in a Face Boundary Layer. Generalization of Experimental Data and Comparison with Calculation. Convective heat exchange in a face boundary layer was studied in a vortex chamber of diameter D = 200 mm and an identical height L = 200 mm (Fig. 1). The transfer of heat was studied at an undiaphragmed face fabricated of glass-impregnated fabric (glass Textolite), covered with a copper foil of thickness ~50 μm. Parallel grooves were milled into the foil with a width of 0.4 mm so as to form a current-conducting strip exhibiting a width of a = 3 mm and an overall length of ~12 m. The face wall was heated by means of passing a direct electric current through the copper

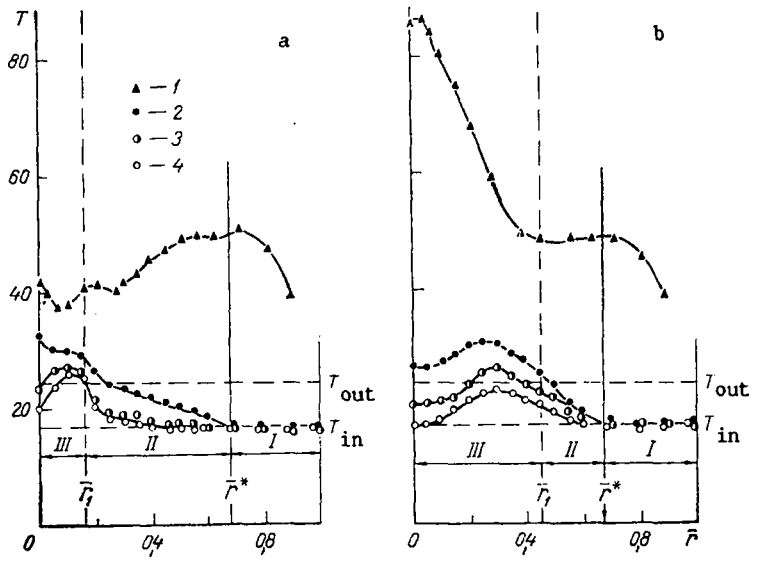

Fig. 2. Distribution of temperatures in the face wall and in the core of the flow along the radius of the vortex chamber (Re_c = $2 \cdot 10^5$, Ro = 0.07, q_w = 6.1 kW/m^2): a) $\bar{r}_1$ = 0.15; b) $\bar{r}_1$ = 0.45; 1) T_w; 2-4) T_0 for z = 10, 100, and 190 mm, respectively; T, °C.

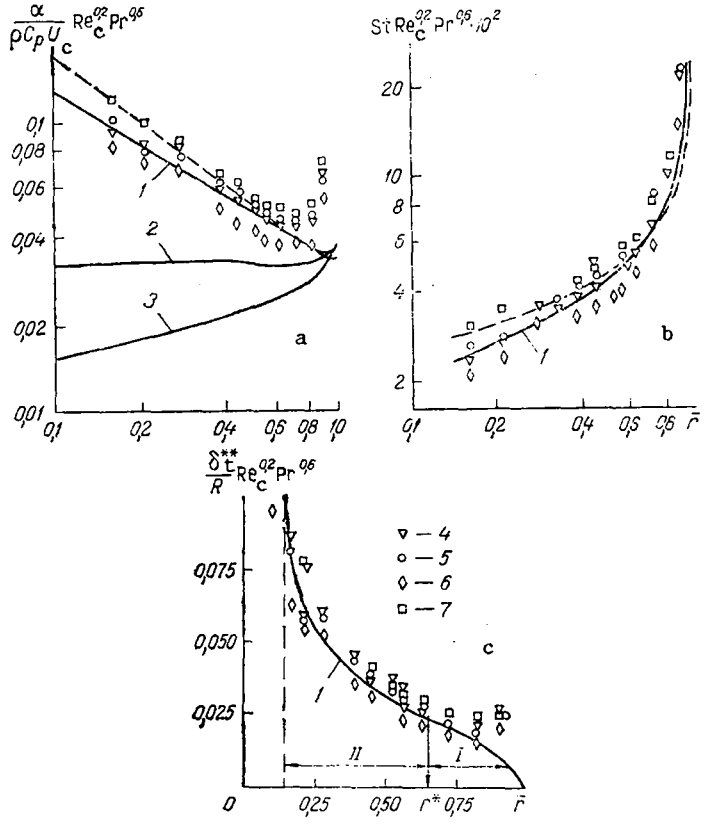

Fig. 3. Change in the coefficient of heat transfer (a), the Stanton number (b), and in the energy loss thickness (c) along the radius of the face wall: 1-3) calculations based on formulas (8)-(10) for m = 1, 0, and −1, respectively; the dashed curves denote calculations for T_w = const and m = 1 [8]; the points represent experiment $\bar{r}_1$ = 0.15; 4) Re_c = $1.13 \cdot 10^5$; 5) $1.27 \cdot 10^5$; 6) $1.53 \cdot 10^5$; 7) $2 \cdot 10^5$.

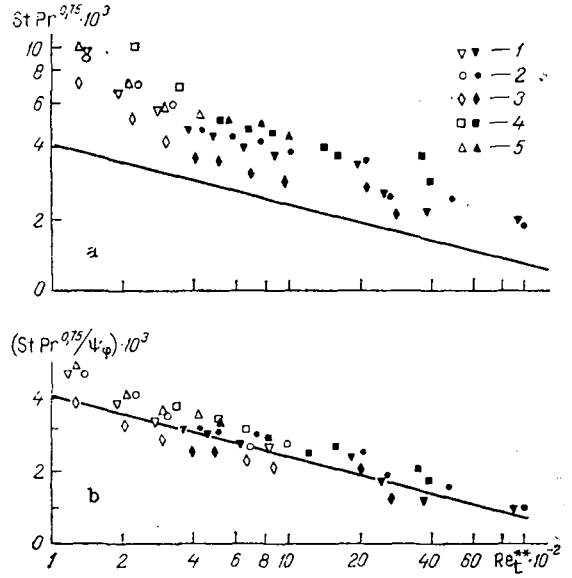

Fig. 4. Law governing transfer of heat in a face boundary layer; the solid line denotes $St = 0.0128Re_t^{**-0.25}Pr^{-0.75}$; the open circles denote the flowthrough zone; the solid circles denote the non-flowthrough zone; Ro = 0.07, $\bar{r}_1 = 0.15$; 1) $Re_c = 1.13 \cdot 10^5$; 2) $1.27 \cdot 10^5$; 3) $1.53 \cdot 10^5$; 4) $2 \cdot 10^5$; 5) $1.11 \cdot 10^5$; $\bar{r}_1 = 0.45$.

strip. The thermal load in these experiments was varied within limits of q_w = 2-6 kW/m^2. To eliminate heat losses, the outer surface of the face and side cylindrical walls of the chamber were thermally insulated. Analysis of the heat losses from the working surface showed that the total error in this study of the heat transfer did not exceed 10%.

The wall temperature distribution through the radius of the face was measured by means of 16 nichrome–constantan thermocouples positioned within the grooves of the heater. The temperature field outside of the face layer was determined by means of three thermocouples moving along the entire diameter of the chamber; they were situated at a distance z = 10 mm from the upper and lower faces, as well as at the midpoint of the chamber height, z = 100 mm. Moreover, the gas temperature was measured in these experiments both at the inlet to and the outlet from the chamber.

Air was used as the working fluid in these experiments. The air was fed into the chamber through four series of round holes d_0 = 4 mm, drilled tangentially. There were 10 holes in each series; these holes were positioned uniformly through the height of the chamber along the side wall. The gas was ejected through an orifice in the center of the unheated face whose diameter was varied during the experiments, d_1/D = 0.15 to 0.45.

The air flow rate in these experiments varied, and the Reynolds number, determined from the measured value of the circular velocity at the periphery of the chamber, exhibited a range of $Re_c = V_c R/\nu = (0.2\text{-}2.0) \cdot 10^5$, while the value of the Rossby number was $Ro = Q/(V_c R^2) = 0.07\text{-}0.1$.

The temperature distribution of the face wall and in the main volume of the vortex chamber is shown in Fig. 2 for two diameters of the outlet orifice. With the aerodynamic parameters prevailing in these experiments, according to the data of [5], the flowthrough zone I of the chamber is bounded by a radius $\bar{r}^* = 0.67$. Therefore, throughout this entire zone of the chamber the rotating gas above the face boundary layer exhibits a constant temperature equal to the temperature of the gas at the inlet. This is confirmed by results from the measurements of the temperature distribution at three cross sections of the chamber (Fig. 2). In zone II ($\bar{r}_1 < \bar{r} < \bar{r}^*$), where the gas rotates without a radial channel, it is heated as a consequence of the exchange of heat with the near-axial flow formed at the hot wall of the face. With increasing distance through the vortex chamber, the temperature of the gas in zone II and in the region III near the axis is reduced, and this is brought about by the exchange of thermal energy with the peripheral flow. A similar trend is noted in the study of heat exchange between near-axial streams stabilized by a vortex flow [10].

As we can see from Fig. 2, the fundamental difference in the temperature fields with a change in the diameter of the outlet orifice is noted primarily in the zone near the axis. The dimension of the near-axial jet formed as a result of the face flow is correlated with the quantity $\bar{r}_1$, and in this case we observe the same unique features as in the case of blowing air into the near-axial region of the jet [10].

Let us now turn to an analysis and generalization of the obtained results. In processing the experimental data, as the decisive temperature in the core of the flow in zone II we took its value in the cross section z = 10 mm, in direct contact with the external boundary of the face boundary layer whose thickness, based on our estimates, did not exceed $\delta \leq 7$ mm.

The nature of the change in the heat-transfer coefficient, in the Stanton number, and in the energy-loss thickness along the radius of the space surface is shown in Fig. 3. The experimental values of the heat-transfer coefficient and of the integral Reynolds number were determined from the formulas

$$\mathrm{St} = q_w/(\rho C_p U_m \Delta T_0); \quad \mathrm{Re}_t^{**} = \frac{q_w}{\rho C_p \nu \Delta T_0} \frac{1-\bar{r}^2}{2\bar{r}} R, \tag{11}$$

while the distribution of the maximum value of the radial velocity was calculated on the basis of formula (3) which provided excellent agreement with experimental data [5, 8].

As we can see from Fig. 3a, the law governing flow rotation exerts significant influence on the magnitude of the heat-transfer coefficient. It assumes its greatest value in the case of gas rotation with conservation of circulation, while it assumes its least value in the case of quasisolid rotation. Here, for the case Γ = const the heat-transfer coefficient initially falls, subsequently increasing, and its minimum value, as shown by calculation, is found at $\bar{r} = 0.9$. This type of change in α is explained by the mutual influence on this value exerted by the heat-exchange function which diminishes in the direction of the chamber axis and by the thickness of the boundary layer which increases in proportion to the development of the boundary layer. The Stanton number diminishes, as is demonstrated by both theory and experiment (Fig. 3b), with potential rotation of the gas toward the axis, while the energy-loss thickness increases (Fig. 3c). Comparison of calculation and experimental data for all the basic parameters shows them to be in good agreement, with the existing difference in the region adjacent to the side wall explained by the presence of laminar and transitional segments at the onset of face-layer formation, as well as by the additional thermal losses to the side surface. The results of the calculation for the boundary condition T_w = const (the dashed curves in Fig. 3) yielded results close to q_w = const, which is evidence of the conservative nature of the law governing the exchange of heat in the face of changes in boundary conditions.

We then proceeded in the next stage to generalize the experimental data. Figure 4a shows the change in the heat-transfer coefficient for the flowthrough zone I and non-flowthrough zone II of the chamber as a function of the Reynolds number, constructed through the thickness of the energy losses. The experimental data on heat transfer at the face in region III of the outlet orifice were eliminated from the analysis, since in this zone we have a complex restructuring of the face flow into an ascending near-axial stream. As we can see from Fig. 4a, the experimental data derived for various tangential numbers Re_c and outlet-orifice radii $\bar{r}_1$ lie significantly higher (by more than a factor of two) above the heat-exchange law for a plate. Such an intensification of heat exchange in the face boundary layer is a result of the three-dimensionality of the flow. The experimental data processed with consideration of the heat-exchange function Ψ_φ (Fig. 4b), reflecting the influence of the extensiveness of the flow on the transfer processes, are generalized with respect to each other and coincide with the calculated relationship for a standard boundary layer, both in the flowthrough (open circles) and non-flowthrough (solid circles) zones of the vortex chamber.

Thus it has been established experimentally and theoretically that the quantitative relationships governing the development of a thermal boundary layer on interaction of a rotating flow with a face surface can be described by making use of the relationships for the one-dimensional streamlining of a plate. In this case we have to take into consideration the intensification of the heat exchange as a consequence of the three-dimensional nature of the flow Ψ_φ, whose magnitude for turbulent face layers is significant in the case of intense flow rotations.

NOTATION

D and L are the diameter and height of the chamber; $\bar{r}$ is the instantaneous radius; W, V, and U are the axial, circular, and radial velocity components; $\Gamma = Vr$ is the circulation; $\varphi = \arctan U/V$ is the local angle of flow twisting; α is the heat-transfer coefficient; $q = -\rho C_p \overline{W'T'}$ is the turbulent heat flow; $q_w = \alpha \Delta T_0$ is the flow of heat to the wall; $\Delta T = T_w - T$; $\Delta T_0 = T_w - T_0$; $\Theta = \Delta T/\Delta T_0$; $St = q_w/(\rho C_p U_m \Delta T_0)$ is the Stanton number; U_m is the maximum value of the radial velocity through the cross section of the boundary layer; δ and δ_t are the thicknesses of the dynamic and thermal boundary layers; $Re_t^{**} = \rho U_m \delta_t^{**}/\mu$ is the Reynolds number, constructed through the energy-loss thickness; $\delta_t^{**} = \int_0^{\delta_t} \frac{U}{U_m}(1 - \Lambda T/\Delta T_0)$ is the energy-loss thickness; Ψ_φ is the relative heat-exchange function which takes into consideration the effect of the extensiveness of the flow; $Re_c = \rho V_c R/\mu$ is the tangential Reynolds number at the periphery of the chamber; $Ro = Q/(V_c R^2)$ is the Rossby number; Q is the volume flow rate through the chamber. Subscripts: 1) the boundary of the outlet orifice; *) the boundary of the flowthrough zone; m) the maximum value; 0) the flow core, for standard conditions; c) the periphery of the chamber; w) conditions at the wall; t) thermal.

LITERATURE CITED

1. W. Lewellen, D. Ross, and M. Rosenzweig, Rocket Engineering and Astronautics, No. 12, 94-103 (1964).
2. D. Wormley, Theoretical Fundamentals of Engineering Calculations, No. 2, 145-159 (1969).
3. E. P. Sukhovich, Izv. Akad. Nauk Latv. SSR, Ser. Fiz.-Tekh. Nauk, No. 4, 78-88 (1969).
4. T. Kotas, Heat and Fluid Flow, 5, No. 2, 77-87 (1975).
5. É. P. Volchkov, S. V. Semenov, and V. I. Terekhov, Zh. Prikl. Mekh. Tekh. Fiz., No. 5, 117-126 (1986).
6. E. P. Sukhovich and É. Ya. Blum, Izv. Akad. Nauk Latv. SSR, Ser. Fiz.-Tekh. Nauk, No. 5, 65-73 (1970).
7. A. A. Khalatov, K. I. Kapitanchuk, and V. A. Mal'kov, Prom. Teplotekh., 8, No. 2, 11-16 (1986).
8. É. P. Volchkov, S. V. Semenov, and V. I. Terekhov, The Structure of Forced and Thermogravitational Flows [in Russian], Novosibirsk (1983), pp. 61-87.
9. E. Cobb and O. Saunders, Proc. R. Soc. London, 236, No. 1206, Ser. A, 343-351 (1956).
10. É. P. Volchkov, V. I. Terekhov, and Yu. N. Tkach, "Experimental research into the displacement of the near-axial stream with peripheral flow in a vortex chamber," Preprint, AN SSSR, Sib. Otd-nie, In-t Teplofiziki, No. 124-85, Novosibirsk (1985).